



LAMINAR FLAME SPEED MODEL AT THE INITIAL STAGE OF FORMATION DIFFUSION FLAME

Dr. Ahmed Abed Al-Kadhem Majhool¹

¹ Lecturer, Mechanical Engineering Department, College of Engineering, Al-Qadissiya University, E-mail: Ahmidkadhim@yahoo.com

ABSTRACT

This work paid special attention on the laminar flame speed in a piloted methane-air in jet diffusion flame due to the strong nonlinearity of chemical reaction process where an extension for the unsteady laminar flamelet model is required. The purpose for doing that is set for two folds. The partial differential equations for solving the combustion model required the representation of laminar flame speed in it and the advanced combustion modeling which is promising step. The probability density function required the laminar flame speed to be modelled as a function in terms of the mixture fraction to perform the integration. The laminar flame speed model is discussed, and the results are compared with the experimental database with good accuracy. The model specifies the conditional laminar flame speed and the difference against the gas flow velocity.

KEYWORDS

Laminar flame speed, Turbulent combustion, Jet diffusion flame, Unsteady flamelet model

نموذج سرعة اللهب الطباقية في المرحلة الأولية من تشكيل اللهب المنتشر

م. د. احمد عبد الكاظم مجهول

قسم الهندسة الميكانيكية، كلية الهندسة، جامعة القادسية

الخلاصة

أولى هذا العمل اهتماما خاصا على سرعة اللهب الطباقية في احتراق غير مختلط لغاز الميثان نتيجة لقوة عملية التفاعل الكيميائي الغير خطي التي تتطلب امتدادا لنموذج اجزاء اللهب الطباقية الغير مستقر. الغرض من القيام بذلك هو ضبط اثنان من الطيات. المعادلات التفاضلية الجزئية لحل نموذج الاحتراق تحتاج الى سرعة اللهب الطباقية فيه ولنمذجة الاحتراق المتقدم الذي يعتبر الخطوة الواعدة. دالة الكثافة الاحتمالية تتطلب تمثيل سرعة اللهب الطباقية باعتبارها دالة بصيغة نسبة الخليط لاجل أداء متكامل. ناقش البحث نموذج سرعة اللهب الطباقية، وتم مقارنة النتائج مع قاعدة البيانات التجريبية مع دقة جيدة. هذا النموذج يصف انتاج سرعة اللهب الطباقية المشروطة والاختلاف مقابل سرعة تدفق الغاز.

Nomenclature

Symbols	Description
a_s	Strain rate, 1/sec
c_p	Specific heat at constant pressure, kJ/kg.K
$C_{\varepsilon 1}$	Turbulence model constant
$C_{\varepsilon 2}$	Turbulence model constant
C_μ	Turbulence model constant
D	Total derivative
erf	Error function
f_μ	Function of viscous damping
g_i	Gravitational acceleration, m ² /sec
h	Total enthalpy, kJ/kg
k	Turbulent kinetic energy, m ² /sec ²
p	Pressure, N/m ²
P_k	Turbulent production term, m ² /sec ²
Re	Reynolds number
S_L	Laminar flame speed, m/sec
$S_{st,L}$	Stoichiometric laminar flame speed, m/sec
t	Time, sec
T	Temperature, K
u	Local velocity, m/sec
U	Average mean velocity, m/sec
x	Distance, m
Y	Species mass fraction
Z	Mixture fraction

Greek symbols

Symbols	Description
δ	Partial derivative
ε	Rate of turbulent kinetic energy dissipation, m ² /sec ³
μ	Dynamic viscosity, kg/m.sec
μ_t	Turbulent viscosity, m ² /sec ²
ρ	Density, kg/m ³
σ	Prandtl number
τ	Time interval, sec
χ	Scalar dissipation rate, 1/sec
ω	Chemical reaction rate, kg/m ³ .sec

1. INTRODUCTION

According to the usage, the description of the laminar flame speed, which varies with pressure, temperature and mixture composition, where strongly change in internal combustion engines. The laminar flame speed is derived from the context of premixed combustion, therefore the extent of its implementation into the diffusion flame limited. The laminar flame speed which is also named as the laminar burning velocity can be defined as the velocity relative and normal to the flame front which the unburned gases move into the combustion wave and is converted into products under laminar flow conditions.

A simple model for flame propagation was used by [1] to qualitative and quantitative description the effect of cylindrical bomb geometry on the evolution of outwardly propagating flames. They showed the effect of flow field asymmetries on the evolution of an initially spherical flame in the early stages of propagation, where the effect of confinement is nontrivial but weak. Their determination of laminar flame speeds using the conventional constant - pressure technique were investigated experimentally and theoretically. Both experimental and modeling study of laminar flame speed and non-premixed counter flow ignition of n-heptane was studied by [2]. Freely propagating of flame simulations were performed using the Sandia Premix code. The study depicted that, the compared results of laminar flame speed, was reasonably well. The laminar flame speed and extinction stretch rates of conventional (Jet-A) and alternative (S-8) jet fuels have been obtained experimentally by [3].

Experimental results were referred to Jet-A and S-8 exhibit approximately similar flame propagation characteristics but the extinction response was different. On the other hand, the numerical section to model the laminar flame speed was simulated using the PREMIX code, in conjunction with the CHEMKIN and TRANSPORT packages. Theoretically and numerically investigations were utilized from one linear model (the stretched flame speed changes linearly with the stretch rate) and two nonlinear models (the stretched flame speed changes non - linearly with the stretch rate) were used by [4] for extracting the laminar flame speed and Markstein length in the constant-pressure spherical flame method. By considering the accuracy of predication of laminar flame speed and Markstein length from the spherical flame method, he suggested different non-linear models could be e used for different mixtures. In terms of large eddy simulation (LES) using sub-grid scale modeling, a methodology was suggested by [5]. It was proposed that a dynamic correction to molecular diffusion of the progress variable used in a presumed probability density function approach may be determined from the pdf control parameters to ensure the correct laminar flame speed used in with premixed flamelets model.

A model for the laminar flame speed of binary fuel blends was implemented by [6] because of the strong nonlinearity of chemical reaction process and the laminar flame speed of binary fuel blends cannot be computed from the linear combination of the laminar flame speed of each individual fuel constituent. The model showed that the laminar flame speed of binary fuel blends depends on the square of the laminar flame speed of each individual fuel component. Yuhua et al. [7] measured the laminar flame speed and Markstein length of typical syngas/O₂/diluent flames were conducted at normal and elevated pressures and temperatures using a high-pressure combustion chamber. They concluded the effects of Lewis number, flame temperature, pressure and initial temperature were examined on these parameters. Therefore the aim of this work is to investigate the capability of the numerical predications for both dynamic and thermal fields in a turbulent flow by using eddy viscosity turbulence model and unsteady flamelet model.

2. MEAN FLOW EQUATIONS

The governing equations for fluid motion are the Navier-Stokes equations. The flow is assumed to be a steady, turbulent and incompressible flow. When the density of a viscous fluid is constant, the equations are sufficient to model the flow in general form can be described in

terms of the conservation of mass, momentum and mixture fraction equations, which can be written, in Cartesian coordinates as:

Mass conservation equation

$$\frac{D\rho}{Dt} = 0 \quad (1)$$

Momentum conservation equation

$$\frac{D\rho U_i}{Dt} = D_i - \frac{\partial p}{\partial x_i} + \rho g_i \quad (2)$$

Mixture fraction equation

$$\frac{D\rho Z}{Dt} = D_Z \quad (3)$$

Where the total derivative is defined as:

$$\frac{D}{Dt} = \frac{\partial}{\partial t} + U_i \frac{\partial}{\partial x_i} \quad (4)$$

$$D_i = \frac{\partial}{\partial x_i} \left(\mu \frac{\partial U_i}{\partial x_i} - \rho \overline{u_i u_j} \right) \quad (5)$$

and

$$D_Z = \frac{\partial}{\partial x_i} \left(\frac{\mu}{\sigma_Z} \frac{\partial Z}{\partial x_i} \right) \quad (6)$$

Where μ and σ are the fluid viscosity and turbulent Prandtl number respectively.

3. UNSTEADY FLAMELET MODEL

The flamelet concept for turbulent combustion applies when the reaction is rapid compared to the mixture at the molecular level. In this regime, the chemical part of a flame and turbulence can be handled separately. The concept flamelet approaches the Burke-Schumann solution for high Damkhler number and less mechanism (one step chemical reaction). The dissipation rate scale that appears in the equations in flamelet form lists the effects caused by diffusion and convection. This rate is great on smaller scales, but its fluctuations are mainly governed by large scales, which are solved using eddy-viscosity model. The one-dimensional flamelet equations can be written as:

Mass fraction equation

$$\rho \frac{\partial Y_i}{\partial \tau} - \rho \frac{\chi}{2} \frac{\partial^2 Y_i}{\partial Z^2} = \dot{\omega} \quad (7)$$

and energy equation

$$\rho \frac{\partial T}{\partial \tau} - \rho \frac{\chi}{2} \left(\frac{\partial^2 T}{\partial Z^2} + \frac{1}{c_p} \frac{\partial c_p}{\partial Z} \frac{\partial T}{\partial Z} \right) = - \frac{1}{c_p} \sum_{i=1}^N (h_i \dot{\omega}) \quad (8)$$

where τ , c_p , Y_i , h_i and $\dot{\omega}$ are the time, specific heat at a constant pressure, mass fraction, enthalpy and chemical production rate of the i th species, respectively. Here χ is the mixture fraction

scalar dissipation rate for value of Z . Following Pitsch [8] the instantaneous scalar dissipation rate is defined as

$$\chi(Z) = \frac{a_s}{\pi} \exp \left\{ -2[\operatorname{erfc}^{-1}(2Z)]^2 \right\} \quad (9)$$

error function. In the expression above, the scalar dissipation rate at the location where the mixture is stoichiometric is calculated in function of the strain rate by means of the eliminating the physical space parameter a_s , the scalar dissipation rate at stoichiometric condition is presented. Thus, it can be rewritten as:

$$\chi(Z) = \chi_{st} \frac{\exp \left\{ -2[\operatorname{erfc}^{-1}(2Z)]^2 \right\}}{\exp \left\{ -2[\operatorname{erfc}^{-1}(2Z_{st})]^2 \right\}} \quad (10)$$

Where χ_{st} and Z_{st} are the stoichiometric scalar dissipation rate and mixture fraction respectively. The results of the calculations for the solutions of flamelet equations, to create the lamelet library consisting of the values of the species mass fraction, the temperature and chemical source terms.

4. LAMINAR FLAME SPEED MODEL

First of all, an extension of the unsteady flamelet model to include the prediction of the laminar flame speed in the case of non-homogeneous fuel-air mixtures. The requirement to describe the variations of the laminar flame speed S_L with mixture fraction in the flammability limits. The local laminar flame speed can be revised to allow varying with mixture fractions. However through a convenient expression for the mixture fraction. The proposed modeling is based on the existing the fuel into two main zone presented in the form of a piecewise second-order polynomial function according to the flame distribution diagram shown in Fig. 1. The requirement to describe the variations of the laminar flame speed with mixture fraction in the flammability limits are four parameters can be used to describe the laminar flame speed. Z_{lf} , Z_{uf} , Z_{st} and $S_{L,st}$ are the values of mixture fraction at the lower and upper flammability limits, the stoichiometric values of mixture fraction and laminar flame speed respectively. Simply, the temperature behavior in Fig. 1 can give an indication about the constraints that can control the S_L which is accelerated in the lean fuel zone and vanishes at the rich fuel zone due to unburnt fuel. Also it recorded the maximum value at the Z_{st} and features a peak value equal to $S_{L,st}$. It is expressed as:

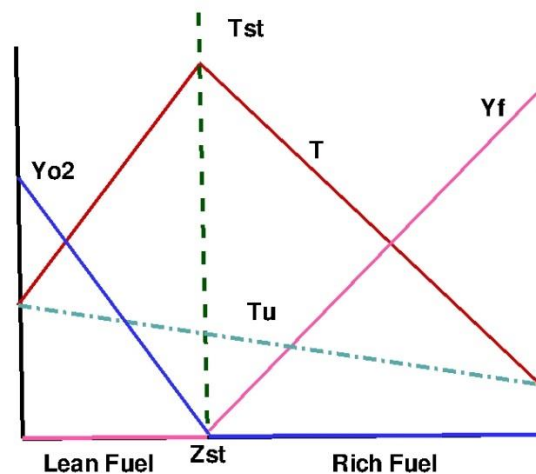


Fig. 1. The Burke - Schumann solution as a function of mixture fraction, Z .

$$S_L = S_{st,L} * \left(1 - \left(\frac{(Z_{st} - Z)}{(Z - Z_{lf})} \right)^2 \right) \quad \text{if } Z_{fl} \leq Z \leq Z_{st} \quad (11)$$

$$S_L = S_{st,L} * \left(1 - \left(\frac{(Z - Z_{st})}{(Z_{uf} - Z)} \right)^2 \right) \quad \text{if } Z_{st} \leq Z \leq Z_{uf} \quad (12)$$

5. THE PROPOSED TURBULENCE MODEL

In this section, the eddy-viscosity models used in this study is presented. The standard $k - \epsilon$ model of [Launder and Spalding \[9\]](#) is a Two Equation model, as already mentioned above, and thus requires two transport equations, one for k (the turbulent kinetic energy) and the other for (its turbulent dissipation rate) ϵ , to describe the turbulence. The low-Reynolds-number $k - \epsilon$ model of [Launder and Sharma \[10\]](#) contains certain modifications which have to be made if one wants to apply this model to near wall regions, where the Reynolds number is low. Therefore the k and ϵ equations are thus:

$$\frac{D(\rho k)}{Dt} = \frac{\partial}{\partial x_i} \left[\left(\mu + \frac{\mu_t}{\sigma_t} \right) \frac{\partial k}{\partial x_i} \right] + \rho P_k - \rho \left[\epsilon + 2\nu \left(\frac{\partial k^{1/2}}{\partial x_i} \right)^2 \right] \quad (13)$$

Where P_k is the production term created by mean shear, defined as:

$$P_k = \nu_t \left(\frac{\partial U_i}{\partial x_i} \right) \quad (14)$$

$$\frac{D(\rho \epsilon)}{Dt} = \frac{\partial}{\partial x_i} \left[\left(\mu + \frac{\mu_t}{\sigma_\epsilon} \right) \frac{\partial \epsilon}{\partial x_i} \right] + C_{\epsilon 1} \rho \frac{\epsilon}{k} P_k - C_{\epsilon 2} f_\epsilon \rho \frac{\epsilon}{k} \quad (15)$$

A commonly used set of coefficients in the standard $k - \epsilon$ model is given below in [Table 1](#).

Table 1: the coefficients in the standard $k - \epsilon$ model

Coefficients	σ_t	σ_ϵ	$C_{\epsilon 1}$	$C_{\epsilon 2}$	C_μ
Values	0.7	1.3	1.44	1.92	0.09

The first modification is the presence of damping functions in order to account for the near-wall region and it is done through introducing a viscous damping function, f_μ , into the turbulent viscosity equation. Therefore,

$$\mu_t = \rho C_\mu f_\mu \frac{k^2}{\epsilon} \quad (16)$$

The function f_μ is used to account for both the true viscous damping at low Reynolds number and then decreases across the viscous sub-layer and the preferential damping of the wall-normal fluctuations as the wall is approached. In this work, the damping function f_μ is given by:

$$f_\mu = \frac{-3.4}{(1 + Re_t/50)^2} \quad (17)$$

Where the turbulent Reynolds number is defined as:

$$Re_t = \frac{k^2}{\nu \epsilon} \quad (18)$$

6. CASE STUDIED

As a validation test case, an experiment well characterized flame of the TNF Workshop [11] has been chosen. It is a piloted methane/air diffusion flame examined experimentally by Barlow and Frank [12] and Schneider [13] as shown in Fig. 2a, where all in all six flames with different Reynolds number have been evaluated. The burner geometry consists of an axis-symmetric jet surrounded by a pilot placed in a co-flowing air stream. The main function of the pilot of this burner is the heat source of hot gases produced by small premixed flames in order to stabilize the main jet at the burner exit. Within this study, only the Sandia C flame is examined. The fuel, which consists of a mixture of 25 vol. % CH_4 and 75 vol. % dry air, resulting in a mass fraction for methane of $Y_{\text{CH}_4} = 0.156$ and air of $Y_{\text{Air}} = 0.844$. The methane is injected through a central nozzle with a diameter of 7.2 mm. The pilot annulus inner diameter is 7.7 mm and its outer diameter is 18.2 mm. The velocity of the lean pilot and the main jet is 0.9 m/sec and 29.7 m/sec respectively. The temperature of the pilot is 1880 K and the mixture fraction is 0.27 and the temperature of the main jet is 294 K. The schematic piloted jet diffusion flame configuration is shown in Fig. 2b.

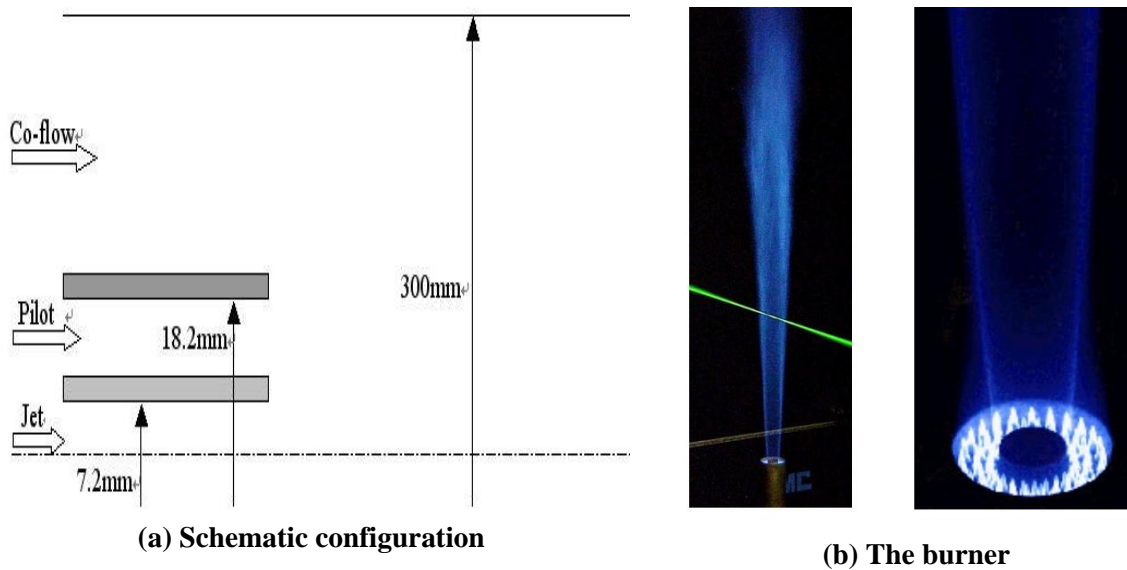


Fig. 2. Sandia flame

7. NUMERICAL TREATMENT

The two dimensional Finite-Volume Method (FVM) is used to discretize the governing equations on structured grids. The Navier - Stokes equations are solving using SIMP LE algorithm of Patankar and Spalding [14]. To discretize the governing equations for fluid flow, the cell-centered finite volume method is selected. In this algorithm the overall solution procedure is iterative and is based on a pressure- correction equation is derived from the discretized equations for continuity, momentum, mixture fraction, turbulent kinetic energy and turbulent dissipation rate. The simulated case is carried out using non-uniform, with 9500 cells,

19195 faces and 9696 nodes in the computational domain shown in Fig. 3. The iterative method which is implemented in the in-house code to solve the discretised equations, is known as Tri-Diagonal Matrix Algorithm (TDMA). The solution of unsteady flamelet model equation is based on solving the two-dimensional unsteady partial differential equations 7 and 8 respectively. A subroutine is called at each iteration to solve the flamelet equations in order to use the local value of the mixture fraction. The two coupled flamelet equations are solved using a second order Crank - Nicholson scheme with an iterative Newton solver. Crank-Nicolson scheme is used for appropriate approximation of the time derivative of the mixture fraction at the first instance. The subroutine uses a Newton solver to solve the non-linear flamelet equations. The Newton solver is guaranteed to converge only if the initial guess is close to the solution. This start profiles file has the solution to the flamelet equations in the flamelet format.

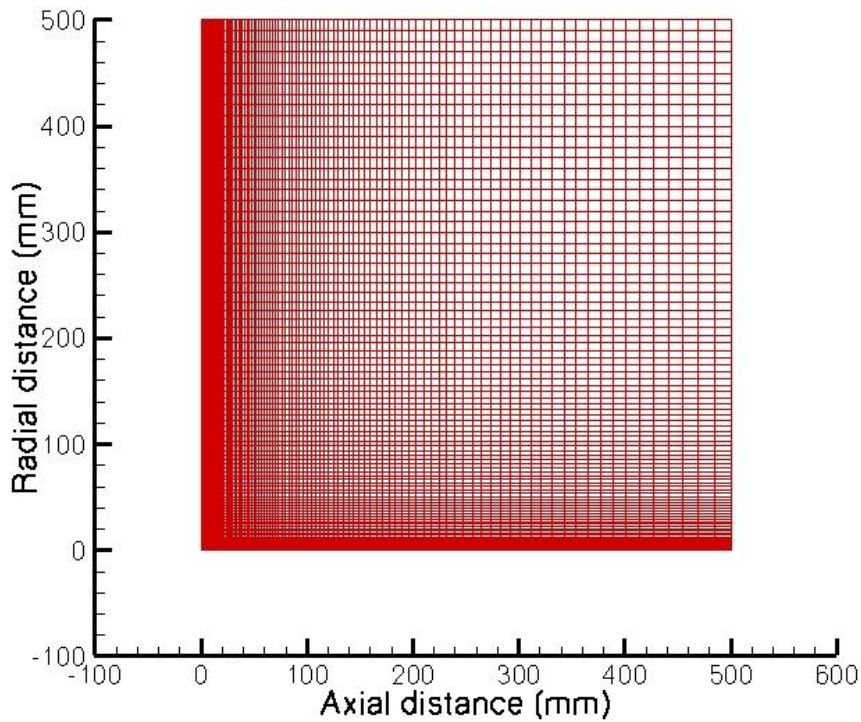


Fig. 3. Computational domain

8. RESULTS AND DISCUSSIONS

Evolution of the behavior of the laminar flame speed for the case of a piloted jet diffusion flame using mixture of methane-air is required a validation. However to achieve this, Fig. 4 shows a comparison between the experimental data of Sandia flame C [12] and the simulated results extracted from the radial profile for the total temperature at axial distance equal to the diameter of the main jet. It can be seen that a good agreement with the experimental data. Although in this regime close to the nozzle, the accuracy of the experimental measurement is not known. Also two points have be mentioned here first, the comparison refers to the matching with the whole shape of the flame. Second, it is observed that the outer edge of the flame is showing sharp and confine flame. This is due using an extra a transport equation for the co-flow for the air which is totally solved separately from the momentum equations. As with all numerical work, it is important to explain the distribution of flame of temperatures that comprise in the jet diffusion flame. Fortunately, there are an experimental works by which to judge the accuracy of these predictions as described above. Therefore, the results shown and discussed here depend

for their explanation on the natural behavior of the structure of the piloted jet diffusion flame. Fig.5 shows the contour plot the numerical predication of total flame temperature using unsteady flamelet model.

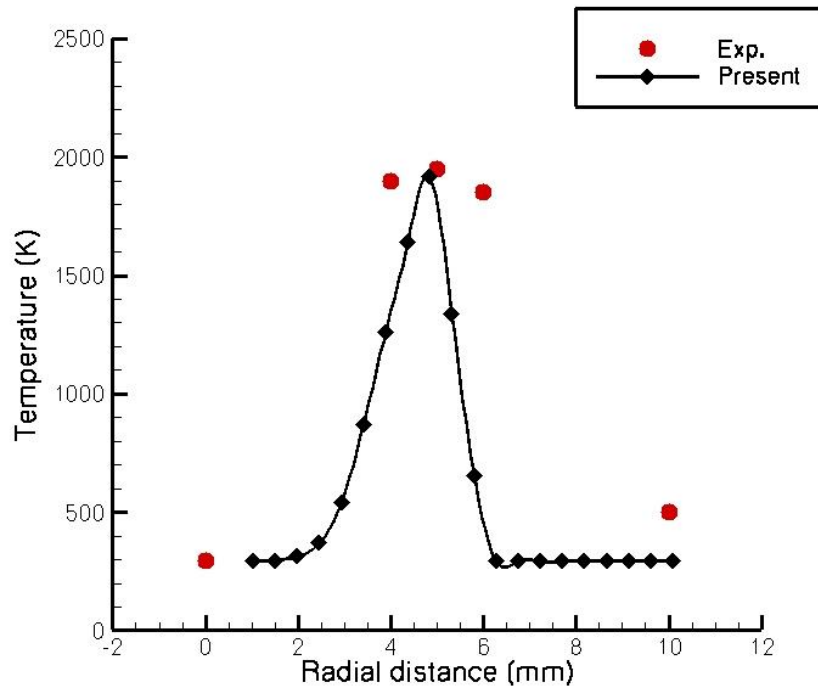


Fig. 4. Comparisons of predicted jet diffusion flame experimental data

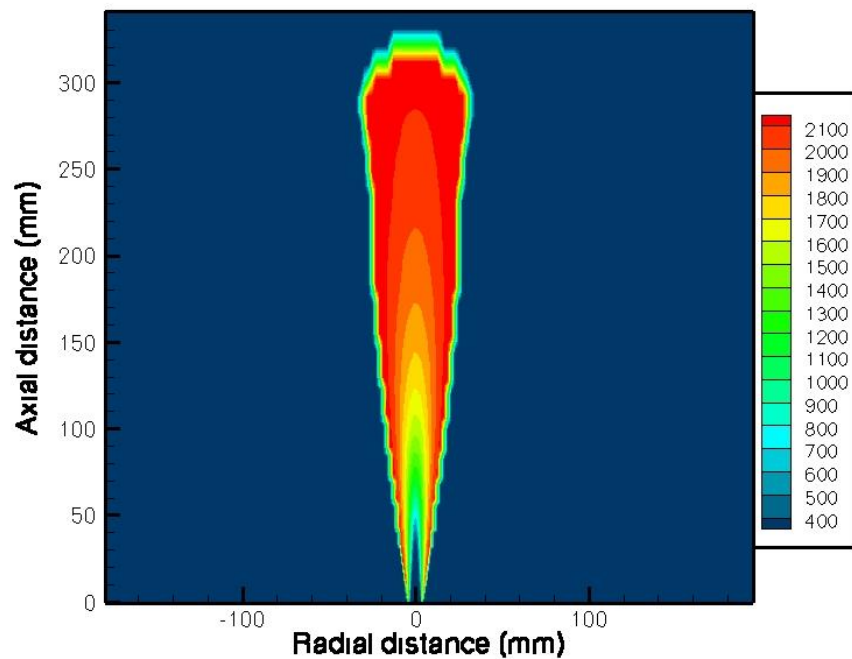


Fig. 5. Jet diffusion flame temperature contour plot

At a low turbulence level at the initial stage of combustion process, both the relative motion of the instantaneous flame speed with respect to the mean flow is appeared to be weakly affected by turbulence and to be mainly controlled by the laminar flame speed and the density ratio. In addition, it should be known that a steady state flame (in both cases laminar and turbulent) develops towards a stationary configuration. At the initial stage of flame formation after ignition, an initial flame proceeds which propagates at the laminar flame speed. Therefore, with the help of the proposed model in this study, the laminar flame speed of pilot jet diffusion flame can be predicted. The base of Fig. 6 corresponds to the initial formation of flame after ignition at time =0.01 sec. The three cutting heights are chosen with reference to this, where $x_1 = 5$ mm, $x_2 = 15$ mm and $x_3 = 30$ mm. As illustrated in the figure, at $x = 5$ mm and $x = 15$ mm. Both axial gas velocity profiles show the same trend. This is due to the inner edge of the flame where outside the flammability limits (due to the presence of rich fuel only) the laminar flame speed is so small that the flame is quenched quickly, as soon as a perturbation occurs. So a value of the laminar flame speed approach to zero m/sec. Whereas it can be seen, the maximum values of the laminar flame speed are reached at stoichiometric conditions at the outer edge of the flame. Whereas at $x = 30$ mm the axial gas velocity profile shows a significant decrease, where a less amount of mass flow rate can be found and the proceeding of the reaction progress.

Fig. 7 shows the gas flow velocity at the initial formation of flame after ignition at time =0.01 sec. Similarly, the three cutting heights are chosen with reference to this, where $x_1 = 5$ mm, $x_2 = 15$ mm, $x_3 = 30$ mm. At $x = 5$ mm and $x = 15$ mm, when fuel is released into ambient air and forms a mixture, that is depending on the gas flow velocity and the co-flow velocity of the fuel-air mixing process, the maximum value of gas velocity is recoded at the centerline. At $x = 30$ mm, the gas velocity is decreased because of the composition of the bulk of the mixture could be lean (below the lower flammability limit) in the case of fast mixing, rich (above the upper flammability limit) in the case of slow mixing, or flammable (within the flammability limits) in the intermediate case.

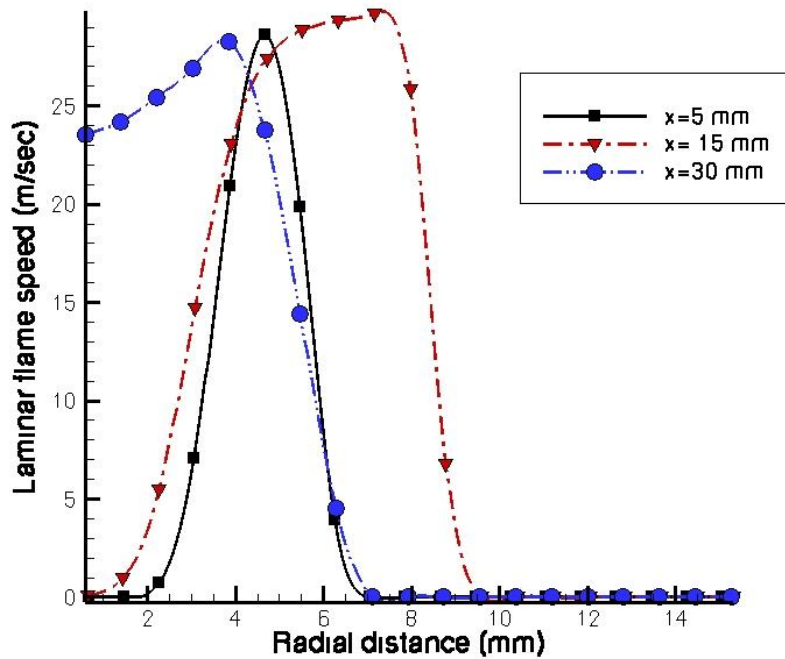


Fig. 6. Prediction of laminar flame speed with radial distance at different axial distances

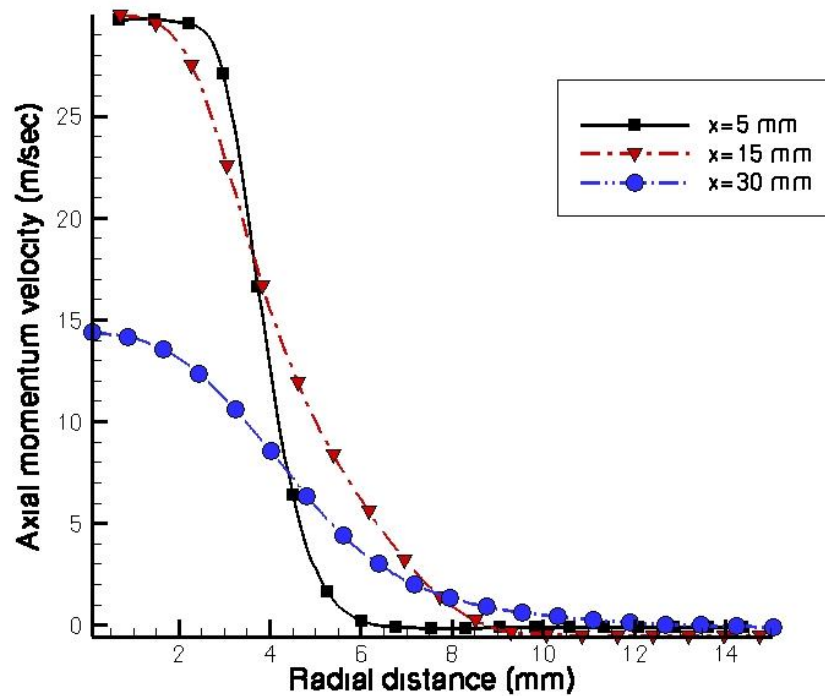
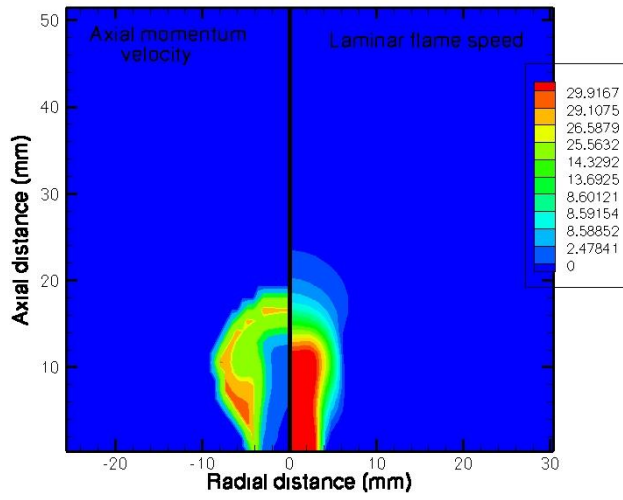
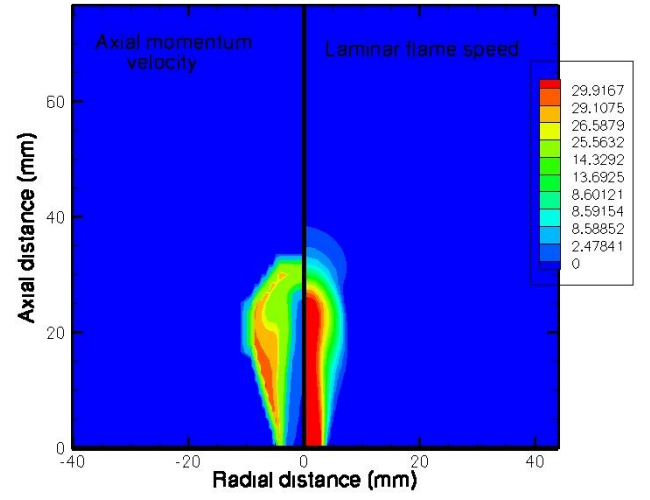


Fig. 7. Prediction of axial gas velocity versus radial distance at different axial distances

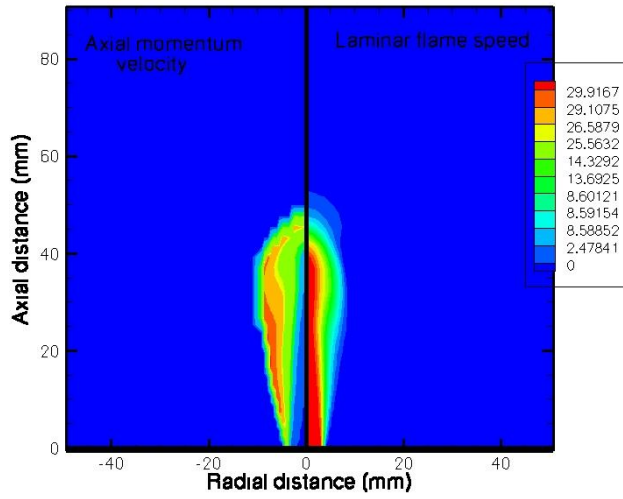
In order to get a fully picture of the proposed study, [Fig. 8](#) shows contour plots of comparison between laminar flame speed and axial gas velocity at different times specified at the initial stages of pilot jet diffusion flame. It can be seen clearly from these plots the difference between the two. One of the main advantages of modeling laminar flame speed is the flame propagation and distribution during the combustion process. Because of the laminar flame speed represents the first stage in turbulent flame development. With this parameter it could be go for the next level of highly investigations, how? For example, the flame radius is calculated through the whole time simulation. However, [Fig. 9](#) does not give a precisely indication about the flame distribution and propagation. Also, the difference is obviously appeared at the final stages where the extra component is added due the turbulent fluctuation of the reactive flow which is out of this study.



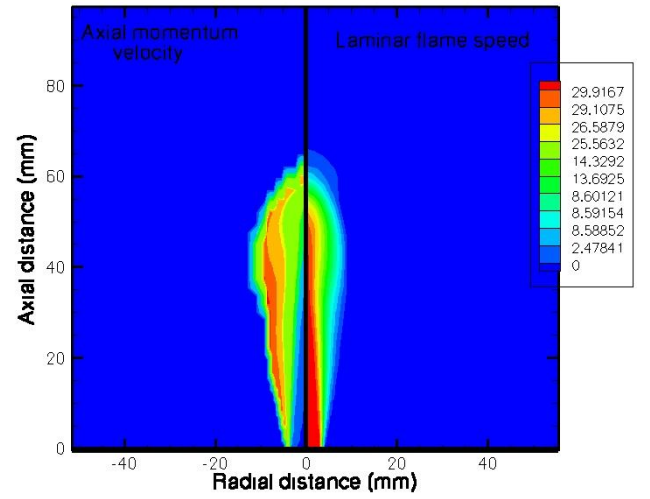
(a) Time=0.01 msec



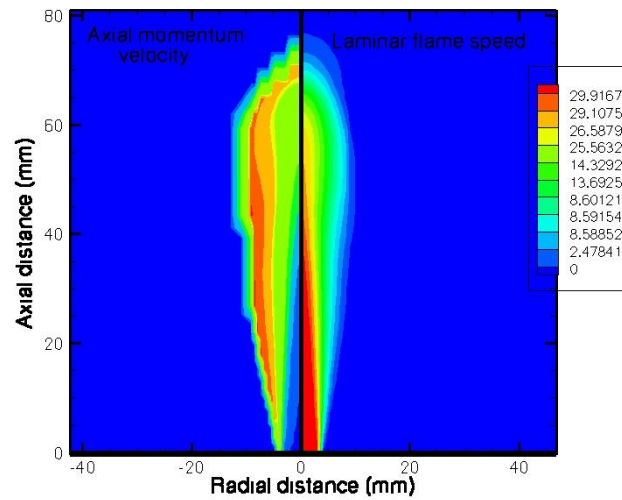
(b) Time=0.02 msec



(c) Time =0.03 msec



(d) Time=0.04 msec



(e) Time=0.05 msec

Fig. 8. Comparisons of laminar flame speed with axial gas velocity at different times

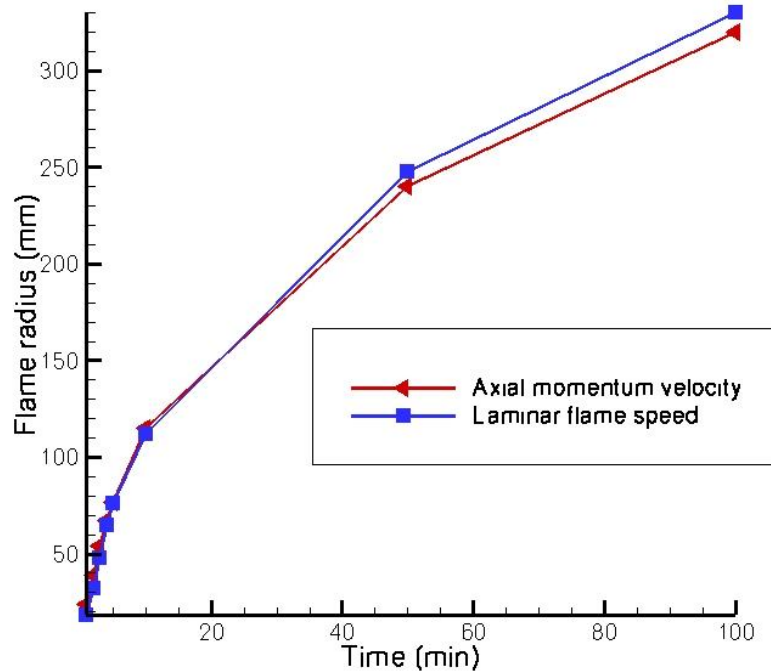


Fig. 9. Evolution of the flame radius for a laminar flame speed and axial gas velocity at different times

9. CONCLUSIONS

In the earlier stages of flame initiation, the flame propagates corresponding to the laminar flame speed. However, as the flame radius grows, the flame structure develops from a laminar flame to a turbulent flame and the burning velocity increases to a fully developed turbulent flame speed. The last can be determined easily from the local turbulence field. As within this work, special attention is paid on the laminar flame speed to extend the unsteady laminar flamelet model.

The purpose for doing that is set for two folds. First the partial differential equations for solving the combustion model need the laminar flame speed in it. Second for advanced combustion modeling which the promising step, the probability density function required the laminar flame speed (as a function) in terms of the mixture fraction for to perform the integration. The laminar flame speed model is discussed, and the results are compared with the experimental database with good accuracy. The model reproduces the conditional laminar flame speed and the difference against the gas flow velocity is specified.

10. REFERENCES

- [1] Michael P. Burke, Zheng Chen, Yiguang Ju, Frederick L. Dryer. Effect of cylindrical confinement on the determination of laminar flame speeds using outwardly propagating flames. *Combustion and Flame* 2009, 156:771 – 779.
- [2] A.J.Smallbone, W. Liu, C.K. Law, X.Q.You, H. Wang. Experimental and modeling study of laminar flame speed and non-premixed counterflow ignition of n-heptane. *Proceedings of the Combustion Institute* 2009, 32:1245 - 1252.

- [3] Kamal Kumar, Chih-Jen Sung, Xin Hui. Laminar flame speeds and extinction limits of conventional and alternative jet fuels. *Fuel* 2011, 90: 1004 - 1011.
- [4] Zheng Chen. On the extraction of laminar flame speed and Markstein length from outwardly propagating spherical flames. *Combustion and Flame* 2011, 158:291 – 300.
- [5] Cindy Merlin, Pascale Domingo, Luc Vervisch. Large Eddy Simulation of turbulent flames in a Trapped Vortex Combustor (TVC) - A flamelet presumed-pdf closure preserving laminar flame speed. *C. R. Mecanique* 2012, 340:917 - 932.
- [6] Zheng Chen, Peng Dai, Shiyi Chen. A model for the laminar flame speed of binary fuel blends and its application to methane/hydrogen mixtures. *International Journal of Hydrogen Energy* 2012, 37:10390 -10396.
- [7] Yuhua Ai, Zhen Zhou, Zheng Chen, Wenjun Kong. Laminar flame speed and Markstein length of syngas at normal and elevated pressures and temperatures. *Fuel* 2014, 137:339 - 345.
- [8] Heinz Pitsch. Unsteady flamelet Modeling of differential diffusion in turbulent jet diffusion flames. *Combustion and Flame* 2000, 123:358 - 374.
- [9] B. E. Launder and D. B. Spalding. *Mathematical models of turbulence*, London Academic press, 1972.
- [10] B. E. Launder and B. I. Sharma. Application of the energy-dissipation model of turbulence to the calculation of flow near a spinning disc. *Letters in Heat and Mass Transfer* 1974, 1: 131 - 138,.
- [11] International Workshop on Measurement and Computation of Turbulent Non- premixed Flames, <http://www.ca.sandia.gov/TNF>, Sandia National Laboratories.
- [12] R.S. Barlow, J.H. Frank. Effects of Turbulence on Species Mass Fractions in Methane/Air Jet Flames. *Symposium (International) on Combustion* 1989, 27:1087 - 1095, The Combustion Institute, Pittsburgh.
- [13] C. Schneider, A. Dreizler, J. Janicka. Flow Field Measurements of Stable and Locally Extinguishing Hydrocarbon- Fuelled Jet Flames. *Combustion and Flame* 2003, 135:185 - 190.
- [14] S.V. Patankar. *Numerical heat transfer and fluid flow*. Hemisphere publishing corporation, Taylor and Francis group, New York, 1980.